IEEE Access
Multidisciplinary | Rapid Review | Open Access Journal

Received November 17, 2019, accepted December 10, 2019, date of publication December 18, 2019,
date of current version January 3, 2020.

Digital Object Identifier 10.1109/ACCESS.2019.2960452

Miniaturized High-Performance Cube-Shaped Filter Made Up of Quasi-TM_{010} Mode Dielectric-Loaded Cavities

LIU-XING ZENG AND FU-MIN LIN
School of Physics and Optoelectronic Engineering, Guangdong University of Technology, Guangzhou 510006, China
Corresponding author: Fu-Min Lin (linfumin@gdut.edu.cn)

This work was supported in part by the Guangdong Science and Technology Program under Grant 2016A010101024, and in part by the Guangzhou Science and Technology Program under Grant 201802020003.

ABSTRACT In this paper, a compact quasi-TM_{010} mode dielectric-loaded bandpass filter with 8th-order pseudoelliptic filtering function and symmetric positioning of 4 transmission zeros is analyzed and designed. The resonant frequency and field components of quasi-TM_{010} mode of a cylindrical dielectric resonator (DR) were first calculated and simulated. Compared to the pure TM_{010} mode, the unloaded Q factor of quasi-TM_{010} mode can increase by 3000 to more than 8000 and then the dimensions of the single DR at 2.595GHz are $\pi \times 34^2 \times 20\,\text{mm}^3$ (using $\varepsilon_\text{r} = 45$). The magnetic coupling and electric coupling between dielectric-loaded cavities are studied and the dielectric window is innovatively proposed to generate electric coupling and to avoid the use of metallic probes that are cumbersome to assemble. In final, a quasi-TM_{010} mode double-layer filter with two pairs of symmetric transmission zeros is designed according to the cubic-like topology and fabricated and tested which exhibits close agreements between the simulated and measured results demonstrating the advantages of low insertion loss, very close-to-band rejections and compact configuration. The proposed filter has great potential for development in 5G mobile communication systems and microwave radar communication systems.

INDEX TERMS Quasi-TM_{010} mode, dielectric resonator, dielectric filter, elliptic filter, transmission zeros.

I. INTRODUCTION

With the development of wireless communication technology, specifications of microwave filters have tended to become very much more severe, which makes them develop in the direction of miniaturization, high selectivity and low loss. Nowadays, dielectric resonator (DR) cavity filters are widely used in mobile communication, radar and satellite systems. Great progress has been made in the study of the $TE_{01\delta}$ mode DR around the 1970s and the research results showed that DR cavity filters have advantages in terms of compact size, low loss and temperature stability [1]–[3]. Many scholars at home and abroad are devoted to the study of miniaturization of dielectric cavity filters. In [4], The theoretical analysis and reasonable estimation of the loaded quality factor of a cavity coupling with coaxial line are first carried out. The Q factor of the $TE_{01\delta}$ mode DR is very high, which leads to the realization of very close-to-band rejections. The Q factor of TM_{010} mode is lower than that of $TE_{01\delta}$ mode, but it is still big enough to achieve the superior performance.

Since the 1980s, single-mode dielectric filters have been investigated and have been widely used in the wireless industry [5]. It has been proved that when a waveguide cavity is loaded with a high-permittivity dielectric material ($\varepsilon_r > 30$), its size is significantly reduced. The higher the ε_r, the smaller the dimensions of the dielectric-loaded cavity. It is well known that bandpass filters using TM_{010}-mode DRs had been first reported by Kobayashi in [6], where the edges of the circular dielectric rod connected to the metallic enclosure. It is shown that no spurious response in the octave band, relative bandwidth of 6 % or more and the unloaded Q is up to 2800 at 6GHz. a $TM_{01\delta}$ mode dielectric rod resonator placed coaxially in a TM_{01} cutoff circular waveguide was discussed in [7], and it is found that this resonator compares favorably to a conventional $TE_{01\delta}$ mode dielectric resonator, particularly for realization of a high unloaded Q. Prof. Zaki

The associate editor coordinating the review of this manuscript and approving it for publication was Kai-Da Xu.

analyzed the characteristic of the combline dielectric resonator [8]. A quasi-TM_{010} mode is supported with a dielectric rod with one [8] or two [7], [9] ends open circuited in a metallic cavity. Multi-mode resonators provide the possibility to implement elliptic and pseudoelliptic filter response with a minimum number of resonators; therefore, further size reduction [10]–[12].

The size of quasi-TM_{010} mode DR is bigger than that of pure-TM_{010} mode DR, but it is smaller than the size of $TE_{01\delta}$ mode DR, and the unloaded Q is improved compared to the pure-TM_{010} mode DR. In [13], the novel double-layer cavity filter is analyzed to provide theoretical and technical support for the development of the more-layer cross-coupling cavity filters. In [14], a cubic pure TM_{010} mode DR filter is designed and optimized for high performance and compact size. The sizes of single-mode dielectric filters are considered larger than that of multi-mode dielectric filters, but they are easy to process and tuning with better temperature stability and structural stability. This can be a simple task in single-mode filters due to the disappearance of spurious couplings between resonances, thus reducing the design complexity and cost.

In this paper, taking the eight-pole quasi-TM_{010} mode filter as design example, the 8 DRs were divided into two layers to form a $2 \times 2 \times 2$ cubic-like structure. The designed filter has good performance and the proposed structure is very attractive to design miniaturized filters for wireless communication systems.

II. ANALYSIS OF QUASI-TM_{010} MODE DR

A. QUASI-TM_{010} MODE AND RESONANT FREQUENCY

Fig. 1 shows the configuration of the quasi-TM_{010} mode cylindrical DR. Variables a and $L-l_1$ are the radius and height of the solid DR with the relative permittivity ε_r, respectively, and b and L denote the radius and height of the metallic cavity respectively. For TM_{010} mode cylindrical DR, as illustrated in [15], both circular surfaces of a dielectric rod are in contact with the metallic enclosure. In [16], the resonator shown in Fig. 1 is used to design triple-mode DR filters with significant size reduction. The basic operation of the TM_{010} mode can be explained as follows. The DR is considered as a short length, L, of dielectric waveguide short at both ends. Since the propagation constant of the electromagnetic wave propagating in the z-axis direction is equal to zero,

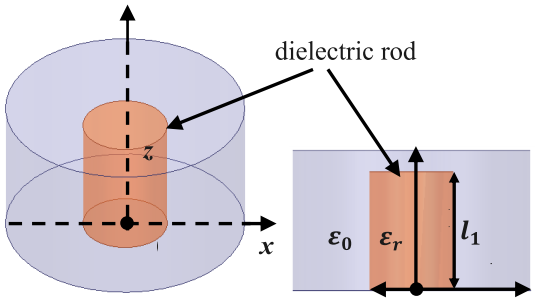

FIGURE 1. Geometry of a quasi-TM_{010} mode cylindrical DR.

the resonant frequency of the resonator is independent of the height L and the magnitude of the field is uniform along the z-axis.

For quasi-TM_{010} mode cylindrical DR, one of the circularsurfaces of a dielectric rod is in contact with the metallic enclosure, another circular surface is very close to the metallic enclosure to ensure that the first dominant mode is quasi-TM_{010} mode. In order to simplify the calculation, the transverse electric field can be ignored, and only the longitudinal electric field exists. In this case, the DR can be divided into three regions each of which has an equal longitudinal electric field amplitude as show in Fig. 2 Since the E-field is mainly concentrated in I and II regions and very weak in III region, it can be approximated that there is only longitudinal electric field in the dielectric-loaded cavity.

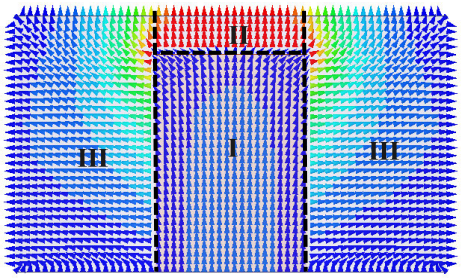

FIGURE 2. E-field of quasi-TM_{010} mode simulated by the full-wave simulation software.

For the TM modes, $H_z = 0$ and the general solution for E_z in the cylindrical dielectric cavity can then be written as

$$E_z = [AJ_0(k_c\rho) + BN_0(k_c\rho)]\, e^{\pm j\beta z} \tag{1}$$

where $J_0(x)$ and $N_0(x)$ are the Bessel functions of first and second kinds respectively, A and B are constants, and k_c is defined as the cutoff wave number, $k_c^2 = k^2 - \beta^2$.

As shown in Fig. 2, E_{z1}, E_{z2} and E_{z3} represent the E-field, $H_{\emptyset 1}$ and $H_{\emptyset 2}$ and $H_{\emptyset 3}$ represent the magnetic field in I, II and III regions, respectively. E_{z1} remains unchanged along the z-axis ($\beta_1 = 0$), while E_{z2} decreases exponentially along the z-axis. Therefore, the E_z can be expressed as follows:

$$E_{z1} = AJ_0\left(\sqrt{\varepsilon}_r k_0\rho\right) \tag{2}$$

$$E_{z2} = \varepsilon_r AJ_0\left(\sqrt{\varepsilon}_r k_0\rho\right) e^{-j\beta(z-l_1)} \tag{3}$$

$$E_{z3} = \sum_{n=0}^{\infty} [B_n J_0(k_n\rho) + C_n N_0(k_n\rho)]\cos\left(\frac{n\pi}{L}z\right) \tag{4}$$

Therefore, based on the fundamental theory of the electromagnetic field [17], the transverse fields are

$$H_{\emptyset 1} = \frac{j\omega\varepsilon_0\varepsilon_r}{\sqrt{\varepsilon}_r k_0} AJ_1\left(\sqrt{\varepsilon}_r k_0\rho\right) \tag{5}$$

$$H_{\emptyset 2} = \frac{j\omega\varepsilon_0\varepsilon_r}{\sqrt{\varepsilon}_r k_0} AJ_1\left(\sqrt{\varepsilon}_r k_0\rho\right) e^{-j\beta(z-l_1)} \tag{6}$$

$$\mathrm{H}_{\emptyset 3} = \mathrm{j}\omega\varepsilon_0 \sum_{\mathrm{n}=0}^{\infty} \frac{1}{\mathrm{k_n}} [\mathrm{B_n J_1}(\mathrm{k_n}\rho) + \mathrm{C_n N_1}(\mathrm{k_n}\rho)]\cos\left(\frac{n\pi}{L}z\right) \tag{7}$$

where k_0 is the wavenumber, and β is the propagation constant in the z-axis direction. Besides,

$$k_n^2 = k_0^2 - \beta^2 = \omega^2\sqrt{\mu_0\varepsilon_0} - \left(\frac{n\pi}{L}\right)^2 \tag{8}$$

The boundary conditions can be applied directly to E_z and H_z:

$$E_{z3} = 0, \quad \rho = b \tag{9}$$

$$E_{z3} = \begin{cases} E_{z1} & \rho = a \text{ and } 0 \le z \le l_1 \\ E_{z2} & \rho = a \text{ and } l_1 \le z \le L \end{cases} \tag{10}$$

$$H_{\emptyset 3} = \begin{cases} H_{\emptyset 1} & \rho = a \text{ and } 0 \le z \le l_1 \\ H_{\emptyset 2} & \rho = a \text{ and } l_1 \le z \le L \end{cases} \tag{11}$$

Equation (10) and (11) can be established by Fourier transform, so they can be written as follows

$$B_0 J_0(k_0 b) + C_0 N_0(k_0 b) = 0 \tag{12}$$

$$\sum_{n=0}^{\infty}\left[B_n J_0(k_n a) + C_n N_0(k_n a)\right] = A J_0\left(\sqrt{\varepsilon_r} k_0 a\right)\sum_{n=0}^{\infty} a_n \tag{13}$$

$$\sum_{n=0}^{\infty}\left[B_n J_1(k_n a) + C_n N_1(k_n a)\right] = \mathrm{A}\sqrt{\varepsilon_r}\mathrm{J}_1\left(\sqrt{\varepsilon_r}\mathrm{k}_0\mathrm{a}\right)\sum_{n=0}^{\infty}\mathrm{b_n} \tag{14}$$

where the a_n, b_n are the coefficients of Fourier transform. Equation (12), (13) and (14) is a set of third-order homogeneous linear equation with an undetermined constant, which have non-zero solution if their coefficient determinant equals zero, that is

$$\begin{vmatrix} 0 & J_0(k_0 b) & N_0(k_0 b) \\ -\mathrm{J}_0\left(\sqrt{\varepsilon_r}\mathrm{k}_0\mathrm{a}\right)\mathrm{a}_0 & J_0(k_0 a) & N_0(k_0 a) \\ -\sqrt{\varepsilon_r}\mathrm{J}_1\left(\sqrt{\varepsilon_r}\mathrm{k}_0\mathrm{a}\right)\mathrm{b}_0 & J_1(k_0 a) & N_1(k_0 a) \end{vmatrix} = 0 \tag{15}$$

where $k_0 = 2\pi f/c$. The derivation of (15) is justified by assuming no field variation both along ϕ and z.

Eqn. (15) can be solved numerically for k_0, which determines the resonant frequency. This solution is approximate since it ignores the transverse field component in the resonator. It yields enough accuracies as long as the gap is small enough (usually accurate enough for practical purposes), and it serves to illustrate the basic behavior of the quasi-TM_{010} mode DRs.

Solving (15) gives the full field component expressions for the TM_{010} mode, where only one undetermined constant is retained, which depends on the amplitude of the transmitted wave in the DR.

As shown in Fig. 3, when $L - l_1 = 0$, the fundamental mode of the DR is pure TM_{010} mode, and when there is an air gap between the dielectric rod and metallic enclosure, the fundamental mode of the DR becomes quasi-TM_{010} mode. As shown in Fig. 3, when $L - l_1 = 0$(pure TM_{010} mode), the calculated results are in good agreement with the simulation results and the resonant frequencies are mainly determined by the radius of the DR. As $L - l_1$ gradually increases, the difference between the calculated results and the simulated results is greater, which is in line with expectations because the transverse field component is ignored in the calculation. The simulated results show that when $L - l_1$ increases to a certain extent, the dominant mode of the DR is no longer quasi-TM_{010} mode.

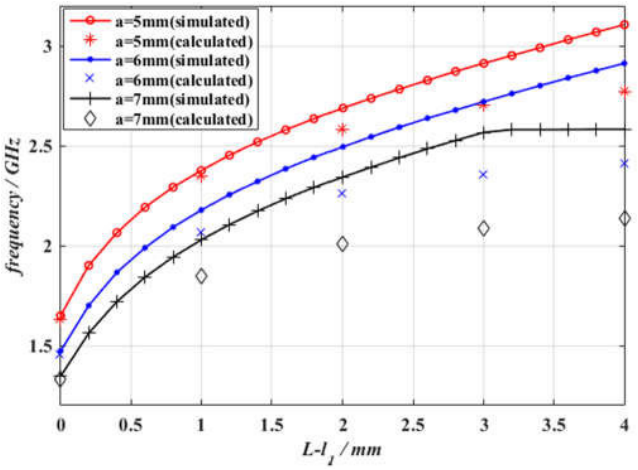

FIGURE 3. Calculated and simulated resonant frequencies of quasi-TM_{010} mode change with the gap of DR ($b = 17mm$, $\varepsilon_r = 45$).

B. UNLOADED Q-FACTOR OF QUASI-TM_{010} MODE

DRs have good unloaded Q-factors. The unloaded Q factors of $TE_{01\delta}$ mode DRs is up to 10000, while that of TM_{010} mode DRs is as high as 5000 under certain conditions. The power loss of a DR generally has two sources: 1. dielectric loss 2. conductor loss. The Q factor of a quasi-TM_{010} mode DR is calculated as follows:

$$\frac{1}{Q_u} = \frac{1}{Q_c} + \frac{1}{Q_d} \tag{16}$$

where Q_c and Q_d correspond to conductor, and dielectric losses, respectively.

The resonant frequencies (2.69GHz) of the pure TM_{010} and quasi-TM_{010} modes are the same by choosing different radius of the dielectric rod (Fig. 4), which ensure that the resonator has a tuning range of 100 MHz. The unloaded Q factor of quasi-TM_{010} mode is about 3000 larger than that of pure TM_{010} mode, which leads to design better insertion loss and out-of-band rejections. The Q factor of the pure TM_{010} and quasi TM_{010} modes changes with the height of the resonator and mainly depends on the Q factor of the conductor loss. The conductor loss decreases with increasing Q factor by increasing the height of the resonator.

III. REALIZATION OF 8-POLE FILTER MADE UP OF QUASI-TM_{010} DIELECTRIC CAVITIES

External coupling, magnetic coupling and electric coupling between resonators and filter topology are analyzed in this section to design a quasi-TM_{010} mode bandpass filter. In this paper, the material of dielectric rod is ceramic with the permittivity of 45±0.5 and tangential loss angle of 0.0001.

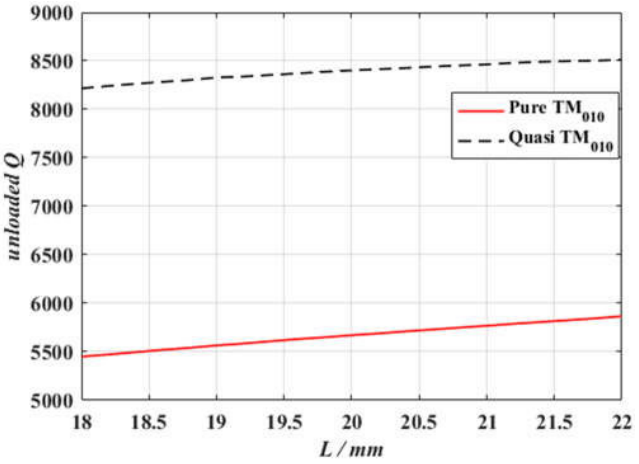

FIGURE 4. Unloaded Q-factor of pure TM_{010} ($a = 2.4mm$, b = 17mm, $\varepsilon_r = 45$, and $L = l_1$) and quasi TM_{010} ($a = 6mm$, $b = 17mm$, $\varepsilon_r = 45$, and $L - l_1 = 3mm$) modes.

On the basis of the former analysis, a novel structure of 8-pole quasi-TM_{010} mode bandpass filter with four symmetric transmission zeros is designed to show the potential of the proposed resonator.

A. FILTER TOPOLOGY DESIGN

The couplings between the resonators is crucial for obtaining a bandpass filter with narrowband and good selectivity. The basic specification for this filter was chosen as 50 MHz ripple bandwidth at 2.595 GHz center frequency with insertion loss less than 1.5 dB and out-of-band rejection of 40 dB at 2.565 and 2.625 GHz, as shown in Table 1.

TABLE 1. Basic specification of the quasi-TM_{010} mode bandpass filter.

SPECIFICATION	EXPECTED VALUE
bandwidth	2570 MHz∼2620 MHz (±0.5MHz)
return loss	≥ 20 dB
insertion loss	≤ 1.5 dB
Out-of-band rejection	≥ 40dB @ 2500 MHz∼2565 MHz ≥ 40dB @ 2625 MHz∼2695 MHz
Power capacity	> 100 W
Dimension (mm)	85×85×50

To achieve such high out-of-band rejection, it requires the design of pseudoelliptic response filters. To locate the finite transmission zeros on both sides, the sign of couplings in one of the cascaded triplets can be altered. In Fig. 5, the numbers represent resonators, inductors represent magnetic couplings with 90° phase shift and capacitors represent electric couplings with -90° phase shift [19]. The topology consists of two cascaded quadruplet (CQ) sections with capacitive cross coupling (① , ②, ③, ④ and ⑤, ⑥, ⑦, ⑧). Each CQ section can generate two transmission zeros above and below the passband. Therefore, two pairs of symmetric transmission zeros can be generated on both sides of the passband.

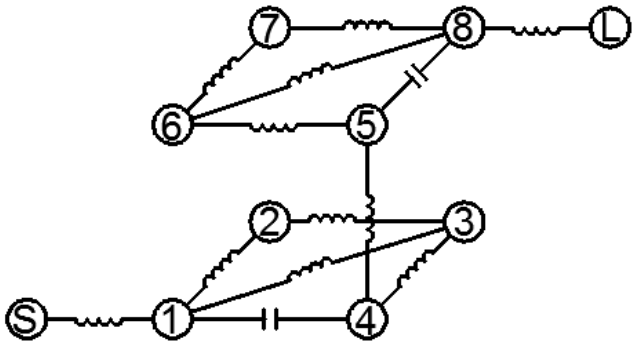

FIGURE 5. The topology of the proposed filter.

According to the coupling matrix synthesis techniques in [18], the normalized coupling matrix is given as follows. The diagonal element in the coupling matrix M_{ii} can be expressed as $\left(f_0^2 - f_i^2\right) / \left(\Delta f f_i\right)$, where f_0, f_i and Δf are the central frequency of the passband, resonant frequency, and absolute BW, respectively, and M is shown at the bottom of this page.

B. EXTERNAL COUPLING AND TUNING MECHANISM

Some commonly used input-output coupling structures in design of coaxial cavity filter are direct tap coupling, loop coupling, capacitive coupling, transformer coupling and so on [19]. It is not suitable to apply direct tap coupling structure to dielectric filters, because the dielectric and metal cannot be in good contact. In this paper, a new external coupling structure similar to a dipole antenna is used, in which the

$$
\mathrm{M} = \begin{bmatrix}
0 & 1.077 & 0 & 0 & 0 & 0 & 0 & 0 & 0 & 0 \\
1.077 & 0 & 0.86 & 0.006 & -0.24 & 0 & 0 & 0 & 0 & 0 \\
0 & 0.860 & -0.01 & 0.751 & 0 & 0 & 0 & 0 & 0 & 0 \\
0 & 0.006 & 0.75 & 0.004 & 0.497 & 0 & 0 & 0 & 0 & 0 \\
0 & -0.24 & 0 & 0.497 & 0 & 0.534 & 0 & 0 & 0 & 0 \\
0 & 0 & 0 & 0 & 0.534 & 0 & 0.434 & 0 & -0.40 & 0 \\
0 & 0 & 0 & 0 & 0 & 0.434 & 0.007 & 0.839 & 0.007 & 0 \\
0 & 0 & 0 & 0 & 0 & 0 & 0.839 & -0.01 & 0.800 & 0 \\
0 & 0 & 0 & 0 & 0 & -0.40 & 0.007 & 0.800 & 0 & 1.077 \\
0 & 0 & 0 & 0 & 0 & 0 & 0 & 0 & 1.077 & 0
\end{bmatrix}
$$

vertical part of the I/O probe along the identical direction excites the quasi-TM_{010} mode, as shown in Fig. 6.

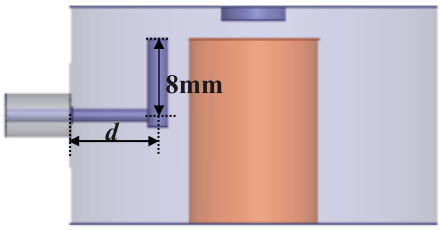

FIGURE 6. External coupling structure of the proposed dielectric filter.

The different external Q factors can be easily obtained by adjusting the length of d, which determines the coupling gap. The longer d, the larger the port coupling coefficient, and the smaller the external Q factor is. Using the method introduced in [20], external Q factor can be extracted. Due to its high permittivity, most of energy is concentrated in the DR.

The tuning screws are necessary because the initial measured results do not always conform to the simulated or desired results. Since the air gap between the dielectric rod and the metal is small, the E-field strength is the largest in this gap. Therefore, positioning tuning screws on cavity cover plate upon the center of the open ends of resonant rod, which is to load resonant capacitor, is the most sensitive tuning method to tune the band center frequency when debugging. Tuning screw is also positioned at the air window between DR cavities to tune pass band and ripple.

C. MAGNETIC COUPLING AND ELECTRIC COUPLING

In the design process of filters, the most important is the design of resonators and coupling structures. If the appropriate coupling structures are chosen to achieve the corresponding coupling coefficients obtained from the filter synthesis, the simulation of the filter can be effectively simplified. The following resonators are TM_{010} mode cylindrical dielectric cavities with a resonant frequency of 2594.9MHz and the normalized coupling coefficients of full wave simulation can be accurately extracted by the multi-port admittance-matrix method of [21]. Fig. 7(a) and Fig. 8(a) shows the magnetic coupling structure with an air window positioned at the center of the two resonators and a tuning screw is positioned at the top of air window to adjust the coupling coefficient. The air window is often used in filter design for magnetic coupling or other mixed coupling and antenna design for broadband impedance matching [22]–[24].

The reason why the magnetic coupling occurs is because the resonant frequency of the air window is higher than the that of the dielectric cavity, resulting in less electric field passing through the air window and most of the magnetic field passing through it. Consider the air window as a rectangular waveguide, the TE_{10} mode is the overall dominant mode of the rectangular waveguide, in which the lowest cutoff frequency is determined by the long side a. Similarly, the coupling coefficient of Fig. 8(a) is mainly controlled by

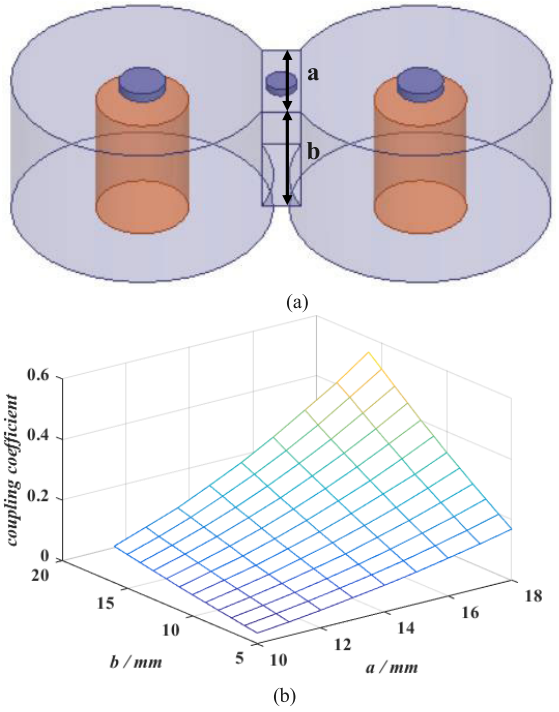

FIGURE 7. (a) Coupling structure between resonators on the same plane with an air window. (b) Normalized corresponding coupling coefficients.

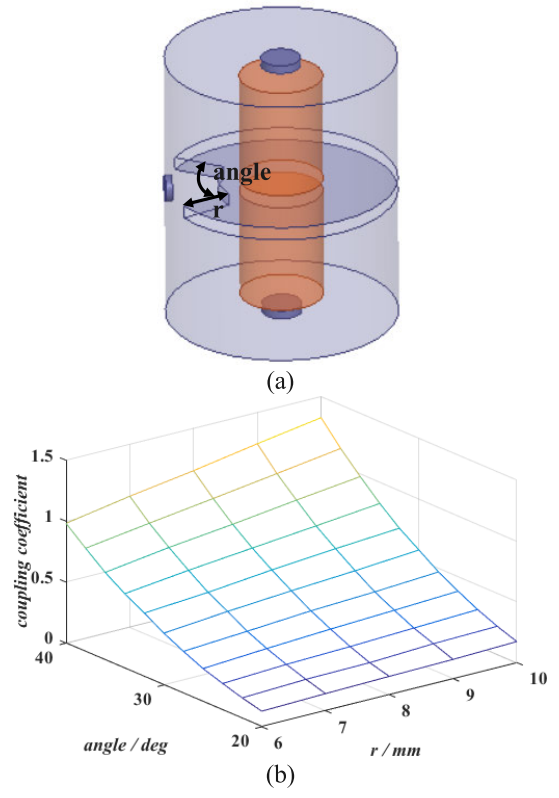

FIGURE 8. (a) Coupling structure of upper and lower resonators with an air window. (b) Normalized corresponding coupling coefficients.

the window angle and it changes slowly with the radius r. Therefore, if the fundamental mode resonance frequency of the air window is increased to be larger than that of the

resonant cavity, the air window is equivalent to the cutoff waveguide, and electrical coupling will occur.

Based on above idea, the concept of a dielectric window was innovatively proposed, which is formed by a thin air window between the two quasi-TM_{010} mode DRs and filling the air window with the same dielectric material as the DR, as shown in Fig. 9(a). For tuning mechanism, the traditional screw tuning method is used. There are two symmetrical screws positioned on both sides of the dielectric window, which is used to adjust the electric coupling coefficient when debugging. The metallic probe is often used to achieve electric coupling coefficients in designing the traditional cavity filter, but the coupling structure is hard to machine and its coupling strength is difficult to adjust because there is little tuning range of tuning screw to tune the pass band and ripple. The metallic probe can produce suitable electrical coupling that vary little with frequency, but it will affect the field distribution of the DR and the unloaded Q value will decrease.

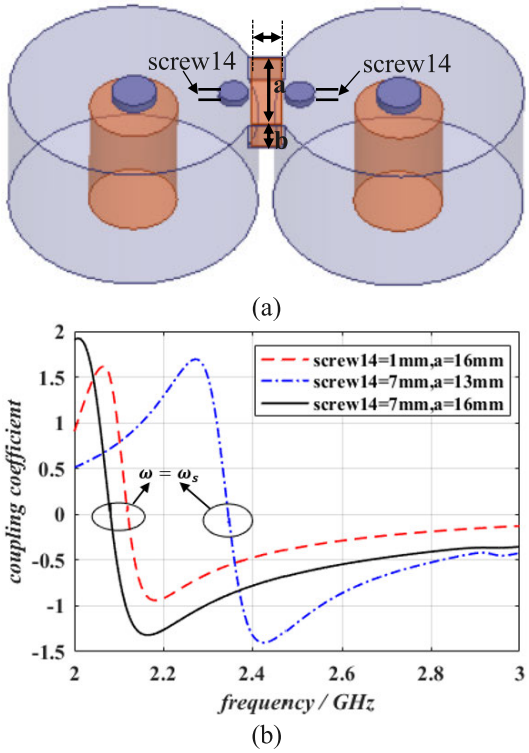

FIGURE 9. (a) Coupling structure of adjacent resonators with a dielectric window. (b) Normalized corresponding coupling coefficients.

As we can see from Fig. 9(b), the longer the screw, the larger the electric coupling coefficient and the width a of the dielectric window becomes shorter, and the curve of the electric coupling coefficient shifts to the right. The way of coupling is changed from magnetic coupling to electric coupling as the working frequency increases and there is a mutation at $\omega = \omega_s$. This phenomenon can be analyzed by the following circuit.

In Fig. 10, it is logical to consider there is a resonant angular frequency ω_s in the dielectric window and think of

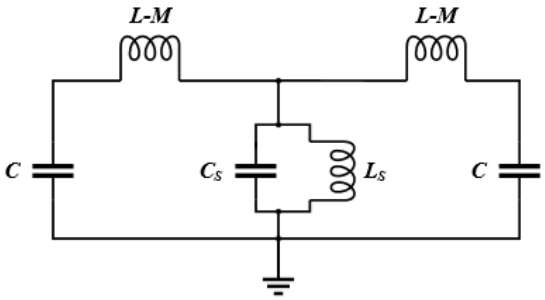

FIGURE 10. Equivalent circuit diagram of the coupling structure (Fig. 11(a)).

the dielectric window as a waveguide. When the working frequency $\omega < \omega_s$, the frequency ω is cut off in the dielectric window and only current can flow through it, so the coupling structure behaves as magnetic coupling. Besides, When the working frequency $\omega > \omega_s$, the frequency ω can be propagated in the dielectric window, so the coupling structure behaves as electric coupling.

The mutual inductance and the mutual capacitance have different sign, so both couplings tend to cancel each other out and the total coupling can be expressed in the form of reactance Z_s.

$$Z_s = \frac{j\omega L_s * 1/(j\omega C_s)}{j\omega L_s + 1/(j\omega C_s)} = j\omega \frac{L_s}{1 - \omega^2/\omega_s^2} \tag{17}$$

$$M = \frac{L_s}{1 - \omega^2/\omega_s^2} \tag{18}$$

where the ω_s correspond to the angular frequency of the dielectric window and the total mutual inductance M is the value after the electric and magnetic coupling cancel each other out. By inserting an electric wall and a magnetic wall, respectively, into the symmetry plane of the equivalent circuit in Fig. 10, two resonant frequencies f_e and f_m can be obtained.

So, the mixed coupling coefficient k can be found to be

$$k = \frac{f_e^2 - f_m^2}{f_e^2 + f_m^2} \tag{19}$$

which clearly indicates that the mixed coupling is related to resonance frequency of the dielectric window and when $\omega = \omega_s$, the value of coupling coefficient k is meaningless which means there is a mutation. It is easy to understand that the larger the slope of the curve, the larger the coupling coefficient changes with the frequency and variable coupling coefficient will affect the filtering effect of the filter.

D. SIMULATED AND MEASURED RESULTS

In this section, a band-pass filter is simulated, fabricated, and measured by using eight quasi-TM_{010} mode resonators with tuning structures.

Fig. 11 shows the photograph of the eight-pole pseudo-elliptic dielectric filter using quasi-TM_{010} mode cylindrical DRs, which utilizes two cascaded quadruplet topologies to generate two pairs of symmetrical transmissions zeros.

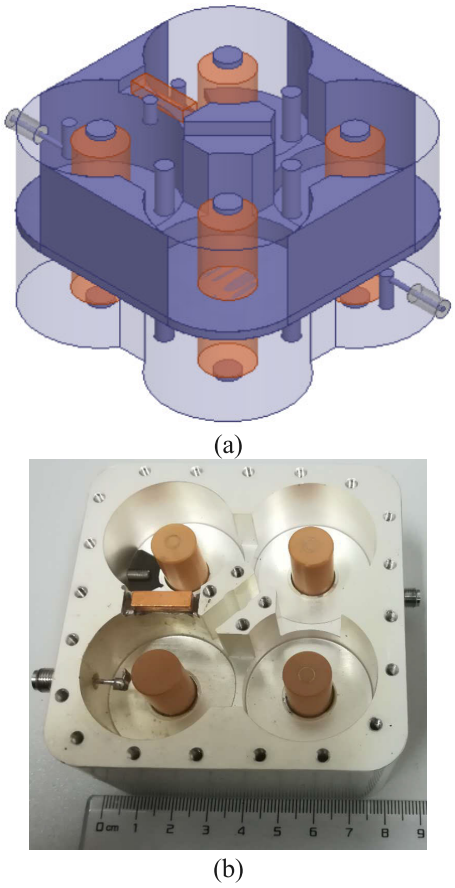

FIGURE 11. Structure of eight-pole quasi-TM_{010} mode dielectric filter. (a) Photograph of the simulated filter. (b) Photograph of fabricated filter.

Using air window to generate magnetic coupling and dielectric window to generate electrical coupling makes the quasi-TM_{010} mode in DR and there is no spurious mode.

Table 2 shows the length of external coupling structure and the length of the tuning screws inserting into the cavity. The parameter d_{01} and d_{8L} represent the lengths of inner conductor of the SMA connectors into the cavities. The parameter a_{12} refers to the width of corresponding coupling structures, where the length of screw is $screw\_l_{12}$, and so on.

TABLE 2. Dimensions of manufactured dielectric filter (unit: mm).

PARAMETER	VALUE	PARAMETER	VALUE	PARAMETER	VALUE
d_{S1}	8.08	screw_l_{12}	11.13	a_{12}, a_{67}, a_{78}	18
d_{8L}	8.13	screw_l_{14}	5.08	a_{14}, a_{58}	14.5
screw_l_1	0.93	screw_l_{23}	11.87	a_{23}	16
screw_l_2	1.11	screw_l_{34}	10.99	a_{34}	14
screw_l_3	1.23	screw_l_{45}	5.83	a_{56}	13
screw_l_4	1.30	screw_l_{56}	11.25	b_{14}	3
screw_l_5	1.33	screw_l_{58}	6.16	b_{58}	4
screw_l_6	1.19	screw_l_{67}	10.29	d_{14}, d_{58}	4
screw_l_7	1.08	screw_l_{78}	10.75	angle	58°
screw_l_8	1.01			r	9

The parameter $screw\_l_1$ refers to the screw length of the first DR, and so on.

To validate the novel topology structure and the dielectric window, the fabricated prototype was measured using an Agilent E5071C ENA RF Network Analyzer. The photograph of the designed dielectric filter is shown in Fig. 11, and the synthesized, simulated and measured return loss and insertion loss are shown in Fig. 12.

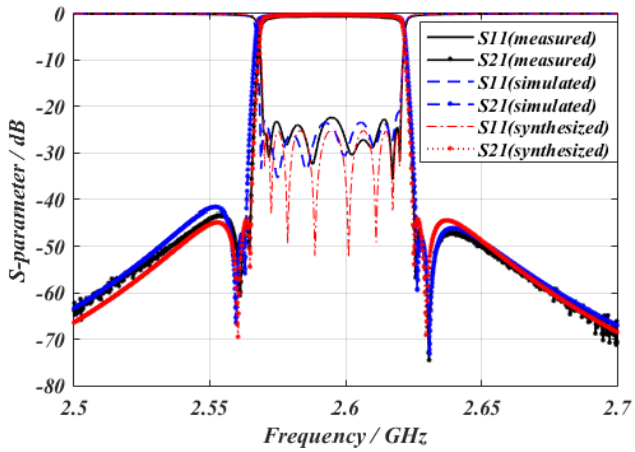

FIGURE 12. Simulated, measured and synthesized S-parameters of the eight-pole quasi-TM_{010} mode dielectric filter in the 2.5GHz to 2.7GHz band.

Fig. 13 shows the broadband response of the designed filter. The first spurious response is at 2.94GHz, about 300 MHz away from the passband, which is suppressed to below 20dB. The higher the frequency, the more the spurious response, but the farther away from the passband. Besides, the band insertion loss was less than 1.5dB, the return loss was less than −20dB with more than 43dB attenuation at 2.565 GHz and more than 41dB attenuation at 2.625GHz, which can meet the specification of 4G base station filter.

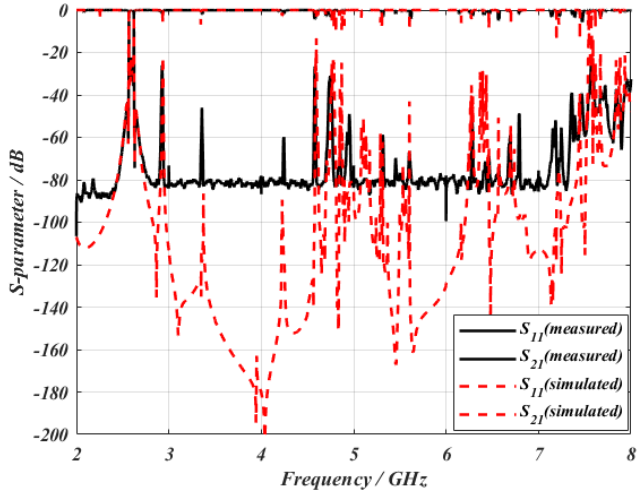

FIGURE 13. Simulated and measured S-parameters of the eight-pole quasi-TM_{010} mode dielectric filter in the 2GHz to 8GHz band.

Table 3 illustrates the comparisons of measured results for several bandpass dielectric-loaded filters. Compared to other dielectric-loaded filters [8], [9], [25], [26], better out-of-band rejections with good insertion loss and return loss can be achieved by proposed designs, small size is also required.

TABLE 3. Comparison to some reported single-band bandpass filters.

Works	Passband (MHz)	S11 (dB)	S21 (dB)	Stopband	Dimension (mm)
Ref. [8] (8-pole)	2583.5~2616.5	17	2	>20dB @ f_1 -7 MHz >20dB @ f_2 +7 MHz	100*50*36
Ref. [9] (10-pole)	3900~4020	20	1	>40dB @ f_1-10MHz >40dB @ f_2+10MHz	121*47*54
Ref. [25] (4-pole)	2575~2625	20	1	>30dB @ f_1-20MHz >30dB @ f_2+20MHz	54*54*17.5
Ref. [26] (8-pole)	2110~2170	20	1.5	>40dB @ f_1-50MHz >40dB @ f_2+6MHz	100*50*25
This work	2570~2620	20	1.5	>40dB @ f_1-5MHz >40dB @ f_2+5MHz	83*83*48

Note: The f_1 and f_2 represent the up and low sidebands respectively.

Moreover, the simulated and measured results of the filter have reached the expected target values, and the measured results are in good agreement with the full-wave simulation and the synthesized results. The filter design and measured results meet high industrial standard. The power capacity of the fabricated filter is tested in rflight NTWPA-2327500 RF power amplifier. The proposed filter has passed the test with an average output power of 53.3dbm (213.8W) for 10 minutes.

IV. CONCLUSION

We analyzed the quasi-TM_{010} mode dielectric resonator and analytically calculated its resonant frequency. Quasi-TM_{010} mode dielectric resonator has a smaller size than that of $TE_{01\delta}$ mode dielectric resonator, and a higher unloaded Q than that of pure- TM_{010} mode dielectric resonator. A new cube-shaped filter topology is designed to offer compact size and a novel dielectric window is applied to generate electric coupling, avoiding the use of metallic probes, which can reduce the difficulty of manufacturing and design complexity. As a validation example, a cube-shaped bandpass filter made up of quasi-TM_{010} mode dielectric cavities has been designed, fabricated and measured. The results show its good performance with very close-to-band rejections and low insertion loss. Our proposed cube-shaped filter and dielectric window are very attractive to designers of designing high-performance and miniaturized filters for wireless communication systems.

REFERENCES

[1] W. H. Harrison, "A miniature high-Q bandpass filter employing dielectric resonators," *IEEE Trans. Microw. Theory Techn.*, vol. MTT-16, no. 4, pp. 210–218, Apr. 1968.
[2] S. B. Cohn, "Microwave bandpass filters containing high-Q dielectric resonators," *IEEE Trans. Microw. Theory Techn.*, vol. MTT-16, no. 4, pp. 218–227, Apr. 1968.
[3] S. Afridi, I. Hunter, and M. Y. Sandhu, "Spurious free non uniform width dielectric loaded filters," in *Proc. 48th Eur. Microw. Conf.*, Madrid, Spain, 2018, pp. 85–88.
[4] F.-M. Lin and Y.-G. Ding, "Approximate formula of the loaded quality factor of doubly reentrant cylindrical cavity coupling with coaxial line," in *Proc. ICMMT 4th Int. Conf. Proc. Microw. Millim. Wave Technol.*, Nanjing, China, 2004, pp. 491–494.
[5] C. Wang and K. A. Zaki, "Dielectric resonators and filters," *IEEE Microw. Mag.*, vol. 8, no. 5, pp. 115–127, Oct. 2007.
[6] Y. Kobayashi and S. Yoshida, "Bandpass filters using TM_{010} dielectric rod resonators," in *IEEE MTT-S Int. Microw. Symp. Dig.*, 1978.
[7] Y. Kobayashi and M. Minegishi, "A low-loss bandpass filter using electrically coupled high-Q TM/sub 01 delta/dielectric rod resonators," *IEEE Trans. Microw. Theory Techn.*, vol. MTT-36, no. 12, pp. 1727–1732, Dec. 1988.
[8] C. Wang, K. A. Zaki, A. E. Atia, and T. G. Dolan, "Dielectric combline resonators and filters," *IEEE Trans. Microw. Theory Techn.*, vol. MTT-46, no. 12, pp. 2501–2506, Dec. 1998.
[9] M. Yu, D. Smith, and M. Ismail, "Half-wave dielectric rod resonator filter," in *IEEE MTT-S Int. Microw. Symp. Dig.*, Fort Worth, TX, USA, vol. 2, Jan. 2004, pp. 619–622.
[10] W.-C. Tang and S. K. Chaudhuri, "A true elliptic-function filter using triple-mode degenerate cavities," *IEEE Trans. Microw. Theory Techn.*, vol. MTT-32, no. 11, pp. 1449–1454, Nov. 1984.
[11] X. X. Yuan, L.-H. Zhou, and J.-X. Chen, "Triple-mode bandpass filter based on silver-loaded ring-shaped dielectric resonator," *IEEE Microw. Wireless Compon. Lett.*, vol. 28, no. 9, pp. 789–791, Sep. 2018.
[12] D. Miek, S. Salzer, and M. Höft, "Realization of cross-coupled X- and Y-shaped dual-mode dielectric resonator filters," in *Proc. Asia–Pacific Microw. Conf. (APMC)*, Kyoto, Japan, 2018, pp. 506–508.
[13] L.-X. Zeng and F.-M. Lin, "Research on the novel double-layer multi-cavity filter," *Chin. J. Electron.*, to be published.
[14] L.-X. Zeng, "A novel cubic TM010 mode cylindrical dielectric cavity filter," in *Proc. Int. Conf. Microw. Millim. Wave Technol.*, Chengdu, China, 2018, pp. 1–3.
[15] L. Pelliccia, F. Cacciamani, C. Tomassoni, and R. Sorrentino, "Ultra-compact filters using TM dual-mode dielectric-loaded cavities with asymmetric transmission zeros," in *IEEE MTT-S Int. Microw. Symp. Dig.*, Montreal, QC, Canada, Jun. 2012, pp. 1–3.
[16] M. S. Bakr, I. C. Hunter, and W. Bösch, "Miniature triple-mode dielectric resonator filters," *IEEE Trans. Microw. Theory Techn.*, vol. 66, no. 12, pp. 5625–5631, Dec. 2018.
[17] D. M. Pozar, *Microwave Engineering*, 3rd ed. Hoboken, NJ, USA: Wiley, 2012, pp. 125–127.
[18] R. J. Cameron, "General coupling matrix synthesis methods for Chebyshev filtering functions," *IEEE Trans. Microw. Theory Techn.*, vol. 47, no. 4, pp. 433–442, Apr. 1999.
[19] J. B. Thomas, "Cross-coupling in coaxial cavity filters—A tutorial overview," *IEEE Trans. Microw. Theory Techn.*, vol. 51, no. 4, pp. 1368–1376, Apr. 2003.
[20] R. S. Kwok and J.-F. Liang, "Characterization of high-Q resonators for microwave filter applications," *IEEE Trans. Microw. Theory Techn.*, vol. 47, no. 1, pp. 111–114, Jan. 1999.
[21] S. Otto, "Full wave coupled resonator filter optimization using a multi-port admittance-matrix," in *Proc. Asia–Pacific Microw. Conf.* Tokyo, Japan: Yokohama Rubber, 2006, pp. 777–778.
[22] F. Zhu, W. Hong, J.-X. Chen, and K. Wu, "Quarter-wavelength stepped-impedance resonator filter with mixed electric and magnetic coupling," *IEEE Microw. Wireless Compon. Lett.*, vol. 24, no. 2, pp. 90–92, Feb. 2014.
[23] Y. Yu, W. Hong, Z. H. Jiang, and H. Zhang, "E-band low-profile, wideband 45° linearly polarized slot-loaded patch and its array for millimeter-wave communications," *IEEE Trans. Antennas Propag.*, vol. 66, no. 8, pp. 4364–4369, Aug. 2018.
[24] K. Gong, W. Hong, Y. Zhang, P. Chen, and C. J. You, "Substrate integrated waveguide quasi-elliptic filters with controllable electric and magnetic mixed coupling," *IEEE Trans. Microw. Theory Techn.*, vol. 60, no. 10, pp. 3071–3078, Oct. 2012.
[25] X. Wang and K. Wu, "A TM_{01} mode monoblock dielectric filter," *IEEE Trans. Microw. Theory Techn.*, vol. 62, no. 2, pp. 275–281, Feb. 2014.
[26] Z. Zhongxiang, C. Chang, and W. Xianliang, "A compact cavity filter with novel TM mode dielectric resonator structure," in *Proc. IEEE Int. Conf. Microw. Technol. Comput. Electromagn.*, Beijing, China, May 2011, pp. 111–113.

LIU-XING ZENG was born in 1993. He received the B.E. degree from the School of Physics and Optoelectronic Engineering, Guangdong University of Technology, Guangdong, China, where he is currently pursuing the M.S. degree in electronic science and technology. His research concerns microwave filters and RF circuits.

FU-MIN LIN was born in 1964. He received the Ph.D. degree from the Institute of Electrics, Chinese Academy of Sciences, in 2003. He is currently a Professor and also a Instructor of graduate students with the School of Physics and Optoelectronic Engineering, Guangdong University of Technology, Guangdong, China. His research concerns high-power microwave devices, microwave filters and RF circuits, and antenna.